

Nitrogen and Oxygen Donors in Nonlinear Optical Materials: Effects of Alkyl vs Phenyl Substitution on the Molecular Hyperpolarizability

Craig M. Whitaker, Eric V. Patterson, Kevin L. Kott, and Robert J. McMahon*

Contribution from the Department of Chemistry and Materials Science Program, University of Wisconsin, Madison, Wisconsin 53706-1396

Received January 26, 1996[⊗]

Abstract: The second-order nonlinear optical response of amine and phenol/ether derivatives (**1–8**) has been evaluated using experimental and theoretical techniques. Electric-field-induced second-harmonic generation (EFISH) measurements establish that *N*-phenyl substitution of 4-nitroaniline (**1**) produces a greater increase in molecular hyperpolarizability than *N*-methyl substitution. In contrast, *O*-phenyl substitution of 4-nitrophenol (**6**) produces a smaller increase in hyperpolarizability than *O*-methyl substitution. Neither the enhancement of hyperpolarizability upon *N*-phenyl substitution nor the differential substituent effect is anticipated on the basis of qualitative arguments. Careful theoretical analysis using semiempirical sum-over-states and finite field calculations provide explanations for both observed effects.

Introduction

Nonlinear optics (NLO) deals with the interactions of applied electromagnetic fields in various materials to generate new electromagnetic fields, altered in frequency, phase, or other physical properties.¹ Organic molecules able to manipulate photonic signals efficiently are of importance in technologies such as optical communication, optical computing, and dynamic image processing.² The basic strategy of using electron-donor and electron-acceptor substituents to polarize the π -electron system of organic materials, thereby creating the possibility of second-order nonlinear optical response, has been recognized for many years.^{3–7} Early efforts focused on simply maximizing the strength of the electron donors and acceptors to achieve increased molecular hyperpolarizability. Marder, Beratan, and Cheng subsequently established that the strength of the electron donor and electron acceptor must be optimized for the specific π -system in order to achieve the maximum hyperpolarizability.⁸ In the current study, we sought to probe, in detail, fundamental relationships between the structure of electron-donor substituents and the molecular hyperpolarizability of second-order nonlinear optical materials.

Amines are commonly used as electron donors in nonlinear optical materials. The effects of substituting amines with alkyl groups have been widely investigated and are well understood.

We have been interested in the effects of substituting amines with unsaturated π -electron groups;⁹ these effects have been neither widely investigated nor well understood.^{9–11} Phenyl substituents can increase molecular hyperpolarizability,^{9–11} a result described as surprising.¹⁰ In the current manuscript, we present a detailed analysis describing the origin of the enhancement observed upon phenyl substitution of nitrogen donors. We develop a conceptual framework wherein the phenyl substituent serves to extend the π -conjugation of the molecule, albeit in a non-traditional manner.⁹ We also examine the influence of alkyl substitution vs phenyl substitution in both nitrogen donors and oxygen donors. We observe a differential effect: again, a result unanticipated on the basis of the conventional wisdom. Our analysis explains this effect in terms of the structural and electronic features inherent in amines **1–5** and phenol/ethers **6–8**.

Background

Because the nonlinear optical response in organic compounds is due to (hyper)polarization of the π electrons, the nonlinear response is of molecular origin.^{3–5} The interaction of a molecule with an external electric field, \mathbf{E} , is typically expressed using one of the two following power series expansions:

$$\mu_{\text{induced}} = \mu_0 + \alpha \cdot \mathbf{E} + (1/2!) \beta \cdot \mathbf{E} \cdot \mathbf{E} + (1/3!) \gamma \cdot \mathbf{E} \cdot \mathbf{E} \cdot \mathbf{E} + \dots \quad (1)$$

$$\mu_{\text{induced}} = \mu_0 + \alpha \cdot \mathbf{E} + \beta \cdot \mathbf{E} \cdot \mathbf{E} + \gamma \cdot \mathbf{E} \cdot \mathbf{E} \cdot \mathbf{E} + \dots \quad (2)$$

where μ_0 is the permanent ground state dipole moment, α is the linear polarizability tensor, β is the first hyperpolarizability

[⊗] Abstract published in *Advance ACS Abstracts*, October 1, 1996.

(1) Shen, Y. R. *The Principles of Nonlinear Optics*; Wiley: New York, 1984.

(2) (a) *Chem. Eng. News* 1996, March 4, 22–27. (b) Eaton, D. F. *CHEMTECH* 1992, 22, 308–316. (c) Kolinsky, P. V. *Opt. Eng.* 1992, 31, 1676–1684. (d) Boyd, G. T. *J. Opt. Soc. Am. B* 1989, 6, 685–692. (e) Tripathy, S.; Cavicchi, E.; Kumar, J.; Kumar, R. S. *CHEMTECH* 1989, 19, 747–752. (f) Eaton, D. F. *Science* 1991, 253, 281–287. (g) Prasad, P. N.; Reinhardt, B. A. *Chem. Mater.* 1990, 2, 660–669.

(3) Williams, D. J. *Angew. Chem., Int. Ed. Engl.* 1984, 23, 690–703.

(4) *Nonlinear Optical Properties of Organic Molecules and Crystals*; Chems, D. S., Zyss, J., Eds.; Academic Press: Orlando, 1987.

(5) Prasad, P. N.; Williams, D. J. *Introduction to Nonlinear Optical Effects in Molecules and Polymers*; Wiley: New York, 1990.

(6) *Materials for Nonlinear Optics: Chemical Perspectives*; Marder, S. R., Sohn, J., Stucky, G. D., Eds.; ACS Symp. Ser. No. 455; American Chemical Society: Washington, DC, 1991.

(7) Long, N. J. *Angew. Chem., Int. Ed. Engl.* 1995, 34, 21–38.

(8) Marder, S. R.; Beratan, D. N.; Cheng, L.-T. *Science* 1991, 252, 103–106.

(9) Whitaker, C. M.; Kott, K. L.; Patterson, E. V.; McMahon, R. J. *Abstracts of Papers*; 206th National Meeting of the American Chemical Society, Chicago, IL; American Chemical Society: Washington, DC, 1993; ORGN 36.

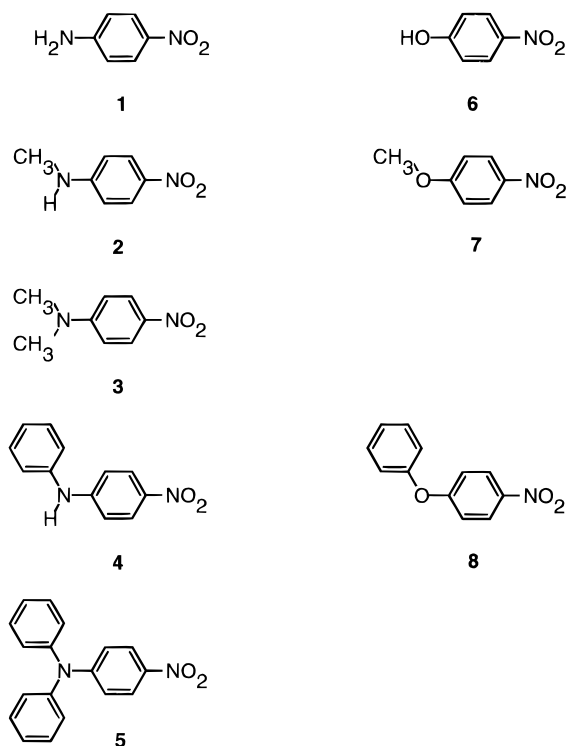
(10) Moylan, C. R.; Twieg, R. J.; Lee, V. Y.; Swanson, S. A.; Betterton, K. M.; Miller, R. D. *J. Am. Chem. Soc.* 1993, 115, 12599–12600. For an important application, see: Verbiest, T.; Burland, D. M.; Jurich, M. C.; Lee, V. Y.; Miller, R. D.; Volksen, W. *Science* 1995, 268, 1604–1606.

(11) Gilmour, S.; Montgomery, R. A.; Marder, S. R.; Cheng, L.-T.; Jen, A. K.-Y.; Cai, Y.; Perry, J. W.; Dalton, L. R. *Chem. Mater.* 1994, 6, 1603–1604.

Table 1. Calculated and Experimental Dipole Moments and Hyperpolarizabilities for 1–9

compd	$\mu^{a,b}$ AM1	μ^a ZINDO	$\mu^{a,c}$ expt	$\ \beta\ ^{d,e}$ MOPAC	$\beta_{\mu}^{d,e}$ MOPAC	$\ \beta\ ^{d,f}$ ZINDO	$\beta_{\mu}^{d,f}$ ZINDO	$\ \beta\ ^{d,g}$ VAMP	$\beta_{\mu}^{d,g}$ VAMP	$\beta_{\mu}^{c,d,h}$ 1064 nm	$\beta_{\mu}^{d,h,i}$ 1907 nm
1	7.3	8.0	7.4	5.5	5.4	11	11	12	12	22	10
2	7.5	8.1	7.7	7.2	7.1	13	12	16	16	24	11
3	7.9	8.4	8.9	9.0	9.0	15	15	20	20	26	13
4	7.1	7.8	6.1	9.7	9.5	16	16	29	28	41	17
5	7.3	7.8	6.5	13	13	23	23	38	38		24
6	5.2	6.0	5.7	2.4	2.3	6.0	5.7	4.9	4.9	5.8	3.6
7	6.0	6.3	5.2	3.3	3.2	6.4	6.1	6.1	6.1	11	5.1
8	6.1	6.2	4.6	4.9	4.8	7.3	7.0	11	11	8.7	4.1
9	7.6	8.3	6.9	16	16	20	20	65	64		14

^a In units of Debye. ^b Both MOPAC and VAMP provide the same computed value of the dipole moment. ^c In 1,4-dioxane. ^d In units of 10^{-30} cm⁵ esu⁻¹. ^e Static hyperpolarizability computed using the AM1/finite field method. ^f Hyperpolarizability computed using the ZINDO/sum-over-states method at 1907 nm. ^g Hyperpolarizability computed using the AM1/sum-over-states method at 1907 nm. ^h Experimental measurement using electric-field-induced second-harmonic generation. ⁱ In chloroform.

Chart 1

tensor, and γ is the second hyperpolarizability tensor.^{1,4,5,12–16} The intrinsic hyperpolarizability $\|\beta\|$ is given by the magnitude of the vector component of the hyperpolarizability (β);¹⁷

$$\|\beta\| = (\beta_x^2 + \beta_y^2 + \beta_z^2)^{1/2} \quad (3)$$

where β_x , β_y , and β_z are the vector components of the hyperpolarizability tensor in the direction of the x , y , and z molecular axes, respectively.

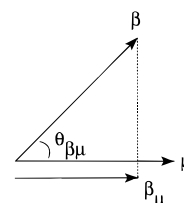
The electric-field-induced second harmonic generation (EFISH) experiment does not measure the intrinsic hyperpolarizability, $\|\beta\|$; it measures the component of the hyperpolarizability in the direction of the dipole moment, β_{μ} . The quantity β_{μ} can also be obtained from the computed hyperpolarizability vector (β) and dipole moment vector (μ) using the following relationships:

$$\cos \theta_{\beta\mu} = \frac{\mu \cdot \beta}{\|\mu\| \|\beta\|} \quad (4)$$

(12) Willetts, A.; Rice, J. E.; Burland, D. M.; Shelton, D. P. *J. Chem. Phys.* **1992**, *97*, 7590–7599.

$$\beta_{\mu} = \|\beta\| \cos \theta_{\beta\mu} = \frac{\mu \cdot \beta}{\|\mu\|} \quad (5)$$

where $\theta_{\beta\mu}$ is the angle between β and μ .



Results

Nonlinear Optical Measurements. Table 1 contains the experimental values of the ground state dipole moment (μ) and the component of the hyperpolarizability in the direction of the dipole moment (β_{μ}) for compounds 1–9. Table 2 contains the electronic absorption maxima (λ_{\max}) for 1–9 in hexane and in chloroform. The molecular hyperpolarizability (β_{μ}) measured for 4-nitroaniline (1, $\beta_{\mu} = 10 \times 10^{-30}$ cm⁵ esu⁻¹ in CHCl₃) at a fundamental wavelength of 1907 nm agrees well with previously reported EFISH measurements.^{18–20} A concentration-dependent analysis of the EFISH data was used to determine the molecular hyperpolarizabilities. The β_{μ} values are not corrected for resonance effects. The hyperpolarizabilities of compounds 1–8 were measured at two different wavelengths, 1064 and 1907 nm, to establish that the EFISH values were internally consistent and to verify that the measured hyperpo-

(13) Different conventions are frequently used to express the induced polarization. In certain instances, the numerical values of the nonlinear coefficients are not directly comparable: values of β differ by a factor of $1/2$, and values of γ differ by a factor of $1/6$. Additional numerical discrepancies may arise from improper treatment of degeneracy factors in different types of nonlinear optical processes.^{12,14} Confusion frequently arises when comparing hyperpolarizabilities calculated using different computational methods and when comparing calculated values with experimental values, because the conventions used are not explicitly stated. For a detailed discussion of this issue, see ref 12.

(14) Orr, B. J.; Ward, J. F. *Mol. Phys.* **1971**, *20*, 513–526.

(15) The EFISH analysis and the VAMP program (AM1/sum-over-states) employ the convention represented by eq 2.¹⁶ The MOPAC finite field subroutine acknowledges the differing conventions and therefore provides the computed values for the hyperpolarizability as β and $\beta/2$ and for the second hyperpolarizability as γ and $\gamma/6$. We report the larger value of β .¹⁶

(16) Kott, K. L.; Whitaker, C. M.; McMahon, R. J. *Chem. Mater.* **1995**, *7*, 426–439.

(17) The quantity $\|\beta\|$ is also commonly referred to as β_{vec} .

(18) Previous EFISH values for 4-nitroaniline: $\beta_{\mu} = 9.2 \times 10^{-30}$ cm⁵ esu⁻¹ in acetone,^{19a} 10×10^{-30} cm⁵ esu⁻¹ in *N*-methyl-2-pyrrolidinone,^{19b} 9.6×10^{-30} cm⁵ esu⁻¹ in 1,4-dioxane.²⁰

(19) (a) Cheng, L.-T.; Tam, W.; Stevenson, S. H.; Meredith, G. R.; Rikken, G.; Marder, S. R. *J. Phys. Chem.* **1991**, *95*, 10631–10643. (b) Cheng, L.-T.; Tam, W.; Marder, S. R.; Stiegman, A. E.; Rikken, G.; Spangler, C. W. *J. Phys. Chem.* **1991**, *95*, 10643–10652.

(20) Teng, C. C.; Garito, A. F. *Phys. Rev. B* **1983**, *28*, 6766–6773.

Table 2. Calculated and Experimental Electronic Absorption Maxima for **1–9**

compd	λ_{\max}^a ZINDO	λ_{\max}^a VAMP	$\lambda_{\max}^{a,b}$	$\lambda_{\max}^{a,c}$
1	320	309	319	345
2	326	313	338	370
3	333	318	352	382
4	337	314	350	380
5	370	335	377	404
6	294	283	284	305
7	295	284	291	303
8	295	279	292	301
9	332	309		374

^a In units of nm. ^b In hexane. ^c In chloroform.

larizabilities are not significantly perturbed by resonance enhancement.

The first set of EFISH experiments establishes the influence of amine substituents on the hyperpolarizability of 4-nitroaniline derivatives. Alkyl substituents produce modest enhancements of the molecular hyperpolarizability, as illustrated by the series 4-nitroaniline (**1**, $\beta_{\mu, 1907} = 10 \times 10^{-30} \text{ cm}^5 \text{ esu}^{-1}$), *N*-methyl-4-nitroaniline (**2**, $\beta_{\mu, 1907} = 11 \times 10^{-30} \text{ cm}^5 \text{ esu}^{-1}$), and *N,N*-dimethyl-4-nitroaniline (**3**, $\beta_{\mu, 1907} = 13 \times 10^{-30} \text{ cm}^5 \text{ esu}^{-1}$). Given this enhancement, dialkylamino substituents are frequently incorporated in organic second-order NLO materials. Perhaps surprisingly, phenyl substitution produces a greater enhancement of the molecular hyperpolarizability than alkyl substitution, as illustrated by the series 4-nitroaniline (**1**, $\beta_{\mu, 1907} = 10 \times 10^{-30} \text{ cm}^5 \text{ esu}^{-1}$), *N,N*-dimethyl-4-nitroaniline (**3**, $\beta_{\mu, 1907} = 13 \times 10^{-30} \text{ cm}^5 \text{ esu}^{-1}$), and *N*-phenyl-4-nitroaniline (**4**, 4-nitrodiphenylamine, $\beta_{\mu, 1907} = 17 \times 10^{-30} \text{ cm}^5 \text{ esu}^{-1}$). Importantly, the larger measured hyperpolarizability of *N*-phenyl-4-nitroaniline (**4**), relative to *N,N*-dimethyl-4-nitroaniline (**3**), does not arise because of a greater degree of resonance enhancement in **4**. The absorption maximum for **4** occurs at slightly shorter wavelength than for **3** ($\lambda_{\max} = 380 \text{ nm}$ vs 382 nm , respectively).

The second set of EFISH experiments establishes the influence of ether substituents on the hyperpolarizability of 4-nitrophenol derivatives. Again, an alkyl substituent produces a modest enhancement of the molecular hyperpolarizability, as illustrated by comparing 4-nitrophenol (**6**, $\beta_{\mu, 1907} = 3.6 \times 10^{-30} \text{ cm}^5 \text{ esu}^{-1}$) and *O*-methyl-4-nitrophenol (**7**, 4-nitroanisole, $\beta_{\mu, 1907} = 5.1 \times 10^{-30} \text{ cm}^5 \text{ esu}^{-1}$). In this instance, a phenyl substituent produces a lesser enhancement of the molecular hyperpolarizability than an alkyl substituent, as illustrated by the series 4-nitrophenol (**6**, $\beta_{\mu, 1907} = 3.6 \times 10^{-30} \text{ cm}^5 \text{ esu}^{-1}$), *O*-methyl-4-nitrophenol (**7**, $\beta_{\mu, 1907} = 5.1 \times 10^{-30} \text{ cm}^5 \text{ esu}^{-1}$), and *O*-phenyl-4-nitrophenol (**8**, 4-nitrodiphenylether, $\beta_{\mu, 1907} = 4.1 \times 10^{-30} \text{ cm}^5 \text{ esu}^{-1}$). Again, the differences in the measured hyperpolarizabilities of **6–8** cannot be attributed to differing degrees of resonance enhancement (Table 1). The trend in the nonlinear optical response for **6–8** was evident in the tables of data previously reported by Cheng et al., but no explanation for this behavior was given.^{19a}

Semiempirical Computations. We previously described our use of the VAMP (AM1/sum-over-states) and MOPAC (AM1/finite field) programs for computing molecular hyperpolarizabilities.¹⁶ Although the VAMP program provided reasonably good predictions for the electronic spectra of the compounds in our earlier study, it typically overestimated the magnitude of $|\beta_{\mu}|$. This raised some concern as to the appropriateness of using the AM1 Hamiltonian in a sum-over-states calculation. In the current study, we addressed this issue by performing sum-

over-states calculations²¹ using Zerner's parametrization of the INDO Hamiltonian.²²

Table 1 contains calculated values for the ground state dipole moment (μ), the magnitude of the first molecular hyperpolarizability ($|\beta_{\mu}|$), and the component of the hyperpolarizability in the direction of the dipole moment (β_{μ}) for compounds **1–8**. Table 2 contains calculated values of the longest-wavelength electronic transition (λ_{\max}) for **1–8**. Optimized structures for **1–8** were obtained at the AM1 level of theory using either MOPAC²³ or VAMP.²⁴ The two methods gave virtually identical geometries. Frequency-independent (static) hyperpolarizabilities were calculated using the finite field method incorporated in MOPAC 6.0.²⁵ (This method cannot treat the frequency dependence of the nonlinear coefficients.) Frequency-dependent hyperpolarizabilities were calculated at 1907 nm using the sum-over-states methods incorporated in Clark's VAMP program²⁶ or in MSI's ZINDO program.^{27,28} The VAMP program utilizes a configuration interaction including single and pair-double excitations (PECI).²⁹ The ZINDO program utilizes a configuration interaction including only single excitations (MECI).³⁰ Brédas et al. demonstrated good correlation between hyperpolarizabilities computed on the basis of AM1 (semiempirical) and 3-21G (ab initio) optimized geometries.³¹ The lowest-energy electronic transitions (λ_{\max}) for compounds **1–8** computed by ZINDO occur at slightly longer wavelength (ca. 10–20 nm) than those computed by VAMP (Table 2).

(21) (a) Kanis, D. R.; Ratner, M. A.; Marks, T. J. *J. Am. Chem. Soc.* **1990**, *112*, 8203–8204. (b) Kanis, D. R.; Ratner, M. A.; Marks, T. J.; Zerner, M. C. *Chem. Mater.* **1991**, *3*, 19–22. (c) Li, D.; Marks, T. J.; Ratner, M. A. *J. Phys. Chem.* **1992**, *96*, 4325–4336. (d) Kanis, D. R.; Ratner, M. A.; Marks, T. J. *J. Am. Chem. Soc.* **1992**, *114*, 10338–10357.

(22) (a) Ridley, J. E.; Zerner, M. C. *Theor. Chim. Acta* **1973**, *32*, 111–134. (b) Ridley, J. E.; Zerner, M. C. *Theor. Chim. Acta* **1976**, *42*, 223–236. (c) Bacon, A. D.; Zerner, M. C. *Theor. Chim. Acta* **1979**, *53*, 21–54. (d) Zerner, M. C.; Lowe, G. H.; Kirchner, R. F.; Mueller-Westerhoff, U. T. *J. Am. Chem. Soc.* **1980**, *102*, 589–599.

(23) Stewart, J. J. P. *Quantum Chemistry Program Exchange*; Indiana University: Bloomington, Indiana; Program 455, Version 6.0.

(24) Rauhut, G.; Alex, A.; Chandrasekhar, J.; Steinke, T.; Clark, T. Universität Erlangen-Nürnberg, 1993.

(25) Kurtz, H. A.; Stewart, J. J. P.; Dieter, K. M. *J. Comput. Chem.* **1990**, *11*, 82–87.

(26) (a) Clark, T.; Chandrasekhar, J. *Isr. J. Chem.* **1993**, *33*, 435–448. (b) Jain, M.; Chandrasekhar, J. *J. Phys. Chem.* **1993**, *97*, 4044–4049.

(27) ZINDO version 95.0; Molecular Simulations, Inc.: San Diego, CA 1995. In the course of the current investigation, we realized that the ZINDO code, as provided by BIOSYM, failed to reproduce electronic absorption spectra, dipole moments, polarizabilities, and hyperpolarizabilities previously attributed to the same algorithm (see: Kanis, D. R.; Marks, T. J.; Ratner, M. A. *Int. J. Quantum Chem.* **1992**, *43*, 61–82). BIOSYM traced the discrepancy to the parametrization for oxygen. The default oxygen parameter is best suited to modeling solvent effects, while a different oxygen parameter is required to model polarizabilities and hyperpolarizabilities. After changing the oxygen parameter, the ZINDO code indeed reproduces all of the data published by Kanis et al. Users of BIOSYM's ZINDO code should note that this subtlety was not recognized until August 1995. Thus, all versions of ZINDO supplied by BIOSYM before that date were not correctly parametrized for computing hyperpolarizabilities of oxygen-containing compounds. The ZINDO values contained in Whitaker, C. M. Ph.D. Dissertation, University of Wisconsin—Madison, 1995, are all incorrect, and have been recomputed for the purposes of this publication.

(28) We used AM1-optimized geometries for the ZINDO computations.

(29) All VAMP hyperpolarizabilities were computed with configuration interaction involving 12 active orbitals (PECI = 12; corresponds to a sum over 73 singlet excited states). Calculations involving 8 and 10 active orbitals (corresponding to 33 and 51 singlet excited states, respectively) established that the sum-over-states calculations reached convergence.

(30) All ZINDO hyperpolarizabilities were computed with configuration interaction involving 145 determinants corresponding to the 145 lowest singlet states.

(31) (a) Brédas, J. L.; Meyers, F.; Pierce, B. M.; Zyss, J. *J. Am. Chem. Soc.* **1992**, *114*, 4928–4929. (b) Meyers, F.; Brédas, J. L.; Zyss, J. *J. Am. Chem. Soc.* **1992**, *114*, 2914–2921. (c) Dehu, C.; Meyers, F.; Brédas, J. L. *J. Am. Chem. Soc.* **1993**, *115*, 6198–6206.

For compounds **1–8**, MOPAC, ZINDO, and VAMP each predict that the major component of the hyperpolarizability tensor lies along the direction of the dipole moment vector, as illustrated by the fact that β_{μ} is nearly equal to $||\beta||$. The MOPAC (AM1/finite field), ZINDO (INDO/sum-over-states) and VAMP (AM1/sum-over-states) computations show qualitative agreement in predicting the major trends in the hyperpolarizabilities for compounds **1–8**. The various computational methods offer rather different predictions for the absolute magnitudes of both $||\beta||$ and β_{μ} . The ZINDO and VAMP calculations of β_{μ} for 4-nitroaniline (**1**, $\beta_{\mu} = 11 \times 10^{-30}$ and 12×10^{-30} cm⁵ esu⁻¹, respectively) at 1907 nm show good agreement with the EFISH value ($\beta_{\mu} = 10 \times 10^{-30}$ cm⁵ esu⁻¹). The MOPAC calculation gives a β_{μ} value ($\beta_{\mu} = 5.4 \times 10^{-30}$ cm⁵ esu⁻¹) ca. one-half of the experimental value.

MOPAC, ZINDO, and VAMP each offer the same qualitative prediction concerning the influence of amine substituents in 4-nitroaniline (**1**): either *N*-methyl substitution or *N*-phenyl substitution will increase the molecular hyperpolarizability (Table 1). Quantitative predictions differ. The MOPAC and ZINDO programs predict that *N*-phenyl substitution and *N,N*-dimethyl substitution produce roughly equal enhancements of the hyperpolarizability. The VAMP program predicts that *N*-phenyl substitution causes a markedly greater increase in hyperpolarizability than *N,N*-dimethyl substitution.

MOPAC, ZINDO, and VAMP each offer the same qualitative prediction concerning the influence of ether substituents in 4-nitrophenol (**6**): either *O*-methyl substitution or *O*-phenyl substitution will increase the molecular hyperpolarizability (Table 1).³² Again, quantitative predictions differ. The MOPAC and VAMP programs both predict that the hyperpolarizability of 4-nitrophenol (**6**) will double upon addition of the phenyl substituent; the ZINDO program indicates a more moderate enhancement of the hyperpolarizability upon phenyl substitution (Table 1).

Discussion

Amines are widely used as electron donors in second-order nonlinear optical materials. Chemists have long known that alkyl substitution of amines increases the electron density at nitrogen, rendering the amine a better electron donor.^{33,34} The alkyl substituent raises the energy of the nonbonding electron pair on nitrogen.^{35,36} In aniline derivatives, the attendant decrease in the HOMO-LUMO energy separation lowers the energy of the first excited state and increases the degree of charge transfer in that state.^{37,38} From the perspective of nonlinear optics, these factors produce a larger molecular

hyperpolarizability.³⁴ The increase in hyperpolarizability is born out experimentally by EFISH measurements (Table 1), can be rationalized qualitatively by the two-level model,^{3–5} and can be predicted in detail by a wide variety of computational methods (Table 1).^{26a,32,39} It is thus very satisfying that these elementary notions, so appealing in their simplicity and apparent predictive power, successfully explain the behavior of alkyl-amino substituents in nonlinear optical materials. As we will develop during the subsequent discussion, application of these simple notions to the analysis of other types of substituent effects in amines and ethers provides misleading predictions that have hindered the exploration of new classes of second-order nonlinear optical materials.

Analyzing the electronic effects of phenyl substitution of an amine is straightforward; interpreting these effects in terms of nonlinear optical response is not. The interpretation involves subtle, offsetting factors that have not been considered in detail previously. Substitution of an amine with a π -electron substituent increases the electron density at nitrogen by the inductive effect, but decreases the electron density at nitrogen by resonance delocalization.³⁷ The net effect is that the π -electron substituent does not significantly perturb the energy of the nonbonded electron pair on nitrogen.³⁷ Nevertheless, the π -electron substituent raises the energy of the HOMO.^{35–38} We now analyze these effects in terms of nonlinear optical response. In the following discussion, it is important to keep in mind that we are considering the effect of adding a phenyl substituent to an amine that already bears one nitrophenyl substituent. From one perspective, substitution of 4-nitroaniline (**1**) with an *N*-phenyl substituent will delocalize electron density away from the donor amine, and thereby might be expected to cause a decrease in hyperpolarizability. Thus, this simple analysis suggests that alkyl substitution increases hyperpolarizability (*vide supra*) while phenyl substitution decreases hyperpolarizability. In our opinion, this scenario accounts for the dearth of *N*-phenyl-substituted NLO materials in the literature. In fact, the first EFISH study of triarylamine NLO materials was not published until 1993; the IBM group described the relatively large measured hyperpolarizabilities as surprising, and offered no detailed interpretation.¹⁰

An alternate view of the effect of phenyl substitution is to consider the additional phenyl substituent as a means of extending the conjugation in the NLO material.⁹ Conjugation length is known to play a critical role in determining second- and third-order nonlinear optical response.^{3–5,19b} In second-order materials, the conjugation length is typically considered as the length of the π -electron system between the electron donor and acceptor substituents (i.e. D- π -A). *N*-Phenyl substitution represents a way of increasing the conjugation length of a molecule (i.e. π' -D- π -A), albeit not in the traditional manner of increasing the conjugation *between* the electron donor and acceptor substituents (i.e. D- π' - π -A). Given these conjugation effects, the interpretation of NLO effects of amines bearing π -substituents is inherently different than the interpretation of NLO effects of amines bearing simple alkyl substituents.

Amines 1–5. EFISH measurements establish that *N*-phenyl substitution of 4-nitroaniline (**1**) produces a greater increase in hyperpolarizability than *N*-methyl substitution (Table 1). MOPAC, ZINDO, and VAMP calculations all predict the qualitative trend, but each predicts a differing degree of enhancement (Table 1). The sum-over-states methods (ZINDO and VAMP) provide insight into the origin of the hyperpolarizability in **1–5**.

Both ZINDO and VAMP calculations indicate that a single, low-energy excited state makes the dominant contribution to

(32) Matsuzawa and Dixon reported very similar results for **6–8** using the MOPAC finite-field method to compute hyperpolarizabilities based on PM3-optimized geometries: Matsuzawa, N.; Dixon, D. A. *J. Phys. Chem.* **1992**, *96*, 6232–6241.

(33) For background and leading references, see: Lowry, T. H.; Richardson, K. S. *Mechanism and Theory in Organic Chemistry*, 3rd ed.; Harper and Row: New York, 1987; pp 296–316.

(34) (a) Dulic, A.; Flytzanis, C. *Opt. Commun.* **1978**, *25*, 402–406. (b) Dulic, A.; Sauteret, C. *J. Chem. Phys.* **1978**, *69*, 3453–3457.

(35) Lias, S. G.; Bartmess, J. E.; Liebman, J. F.; Holmes, J. L.; Levin, R. D.; Mallard, W. G. *J. Phys. Chem. Ref. Data* **1988**, *17*.

(36) Kimura, K.; Katsumata, S.; Achiba, Y.; Yamazaki, T.; Iwata, S. *Handbook of Hel Photoelectron Spectra of Fundamental Organic Molecules*, Japan Scientific Society Press: Tokyo, 1981; Halsted Press: New York, 1981.

(37) Rabalais, J. W. *Principles of Ultraviolet Photoelectron Spectroscopy*; Wiley: New York, 1977; pp 301–336.

(38) In aniline derivatives, the HOMO is mainly π in character, with only a modest contribution from nitrogen.^{35–37} The nonbonding electron pair on nitrogen is *not* the HOMO; in aniline itself, the nonbonding electron pair is HOMO – 2. (This fact is not widely appreciated in the nonlinear optics community.) An alkyl substituent raises the energy of both the nonbonding electron pair and the HOMO.

(39) Daniel, C.; Dupuis, M. *Chem. Phys. Lett.* **1990**, *171*, 209–216.

Table 3. Calculated (ZINDO) Data for the Excited States which May Contribute to $||\beta||$ for *N*-Phenyl-4-nitroaniline (**4**)

singlet state ^a	$\Delta\mu$ (D)	oscillator strength	energy		major transitions (fraction)
			eV	nm	
S ₄	12.5	0.624	3.677	337.2	HOMO → LUMO (0.81) HOMO -1 → LUMO (0.11)
S ₇	3.68	0.116	4.736	261.8	HOMO → LUMO +2 (0.68) HOMO -1 → LUMO (0.11)
S ₁₂	9.13	0.109	5.832	212.6	HOMO → LUMO +3 (0.14) HOMO → LUMO +5 (0.17) HOMO -2 → LUMO (0.33)
S ₁₅	4.85	0.287	6.042	205.2	HOMO → LUMO +2 (0.10) HOMO → LUMO +1 (0.11) HOMO -1 → LUMO +1 (0.22) HOMO -4 → LUMO (0.47)
S ₁₈	6.56	0.498	6.371	194.6	HOMO → LUMO +6 (0.14) HOMO -1 → LUMO +2 (0.16) HOMO -3 → LUMO +1 (0.42)
S ₂₀	3.03	0.645	6.727	184.3	HOMO -1 → LUMO +1 (0.24) HOMO -1 → LUMO +3 (0.24) HOMO -2 → LUMO +2 (0.12) HOMO -3 → LUMO +2 (0.12)
S ₂₁	1.81	0.302	6.803	182.2	HOMO -3 → LUMO +5 (0.52)
S ₂₂	4.48	0.519	6.815	181.9	HOMO -1 → LUMO +3 (0.11) HOMO -1 → LUMO +4 (0.31) HOMO -2 → LUMO +4 (0.13) HOMO -3 → LUMO +5 (0.13)
S ₂₃	3.45	0.680	6.818	181.8	HOMO -1 → LUMO +4 (0.11) HOMO -2 → LUMO +1 (0.23) HOMO -3 → LUMO +5 (0.12)
S ₂₄	8.10	0.259	6.924	179.1	HOMO → LUMO +6 (0.34)
S ₂₇	5.39	0.183	7.044	176.0	HOMO → LUMO +6 (0.18) HOMO -1 → LUMO +2 (0.12) HOMO -3 → LUMO +1 (0.38)

^a The singlet states correspond exactly as listed in the ZINDO/sum-over-states output (S₁ = ground state). All singlet states with oscillator strength >0.1 are listed.

the intrinsic hyperpolarizability of 4-nitroaniline derivatives **1–5**. The computations reveal that these excited states are described predominantly in terms of HOMO-LUMO excitation (Table 3).^{40,41} In **1–5**, the HOMO is localized primarily on the amine nitrogen, and the LUMO is localized on the nitroaryl moiety. The enhancement in hyperpolarizability in going from **1** to **2** to **3** occurs because *N*-methyl substitution raises the energy of the HOMO (Figure 1). As described above, the attendant decrease in the HOMO-LUMO energy separation lowers the energy of the first excited state and increases the degree of charge transfer between the ground state and the first excited state. This explanation is consistent with the observed red-shift in the absorption spectra upon methyl substitution: **1** (λ_{\max} 345 nm), **2** (λ_{\max} 370 nm), and **3** (λ_{\max} 382 nm) (Table 2).

N-Phenyl substitution of 4-nitroaniline (**1**) both raises the energy of the HOMO and lowers the energy of the LUMO in **4** and **5** (Figure 1). These energetic perturbations are more significant than in the case of *N*-methyl substitution, leading to larger red-shifts in the absorption spectra: **1** (λ_{\max} 345 nm), **4** (λ_{\max} 380 nm), and **5** (λ_{\max} 404 nm) (Table 2). In **4**, and to a lesser extent in **5**, the HOMO contains charge density not only on the amine nitrogen, but also on the *N*-phenyl substituent (Figure 2).⁴⁰ The LUMO is localized on the nitroaryl moiety. In the first excited state, charge transfer occurs from *both* the amine nitrogen *and* the *N*-phenyl substituent to the nitroaryl acceptor.⁴¹ The participation of the phenyl moiety in the excited

(40) Molecular orbital diagrams (AM1) and tables of excited states which may contribute to hyperpolarizability for compounds **1–9** are available as supporting information.

(41) ZINDO calculations indicate that the first excited states of **1**, **2**, and **3** can be described predominantly (ca. 95%) in terms of HOMO-LUMO excitation. This is not the case for the first excited states of **4** and **5**. Although HOMO-LUMO excitation remains the largest single contributor (ca. 80%), other electronic configurations cannot be neglected (20%).

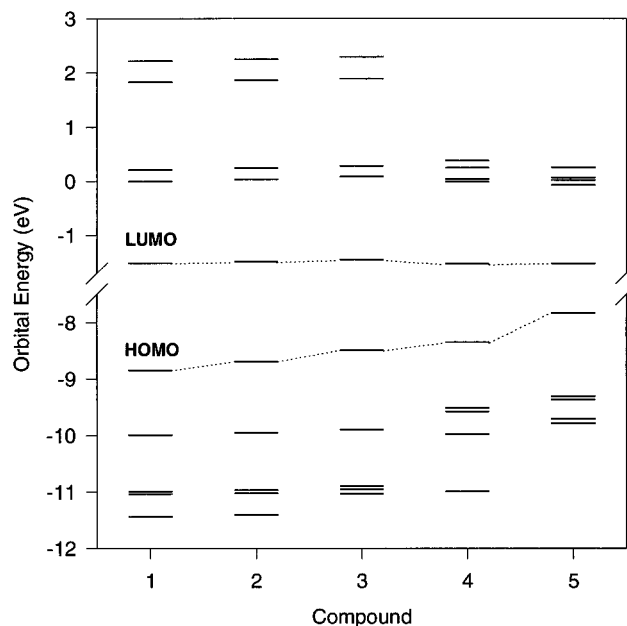


Figure 1. Computed energy levels (ZINDO) for frontier molecular orbitals of 4-nitroaniline (**1**), *N*-methyl-4-nitroaniline (**2**), *N,N*-dimethyl-4-nitroaniline (**3**), *N*-phenyl-4-nitroaniline (**4**), and *N,N*-diphenyl-4-nitroaniline (**5**).

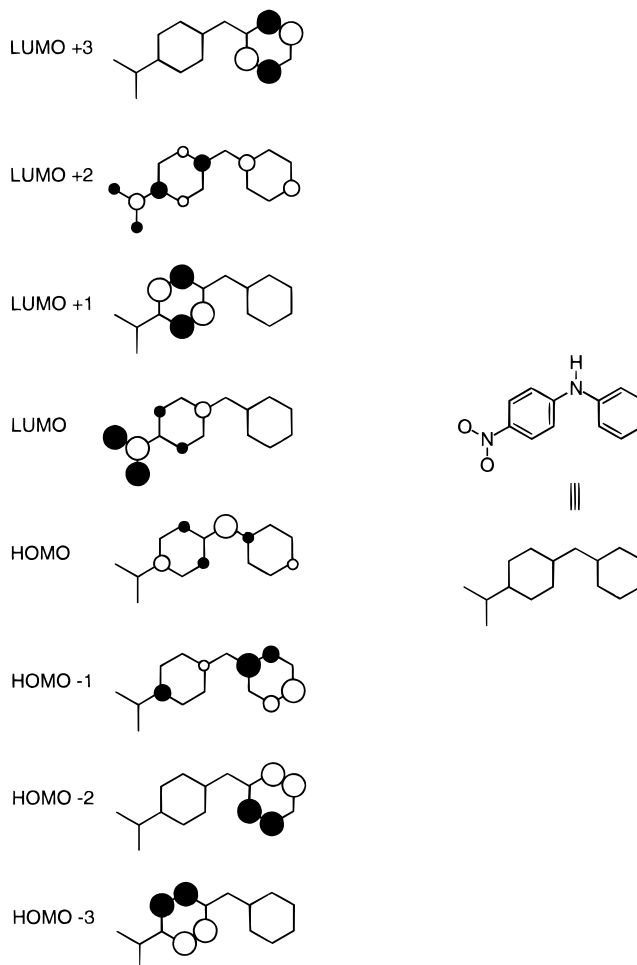


Figure 2. Molecular orbital diagram for *N*-phenyl-4-nitroaniline (**4**). state differentiates the NLO response of *N*-phenyl derivatives **4** and **5** from their *N*-methyl analogs **2** and **3**. The enhancement in hyperpolarizability of **4** and **5**, relative to **1**, **2**, and **3**, arises because of a larger degree of charge transfer between the ground state and the excited state (i.e., *N*-phenyl derivatives **4** and **5**

Table 4. Calculated (ZINDO) Data for the Excited States which May Contribute to $||\beta||$ for *O*-Phenyl-4-nitrophenol (**8**)

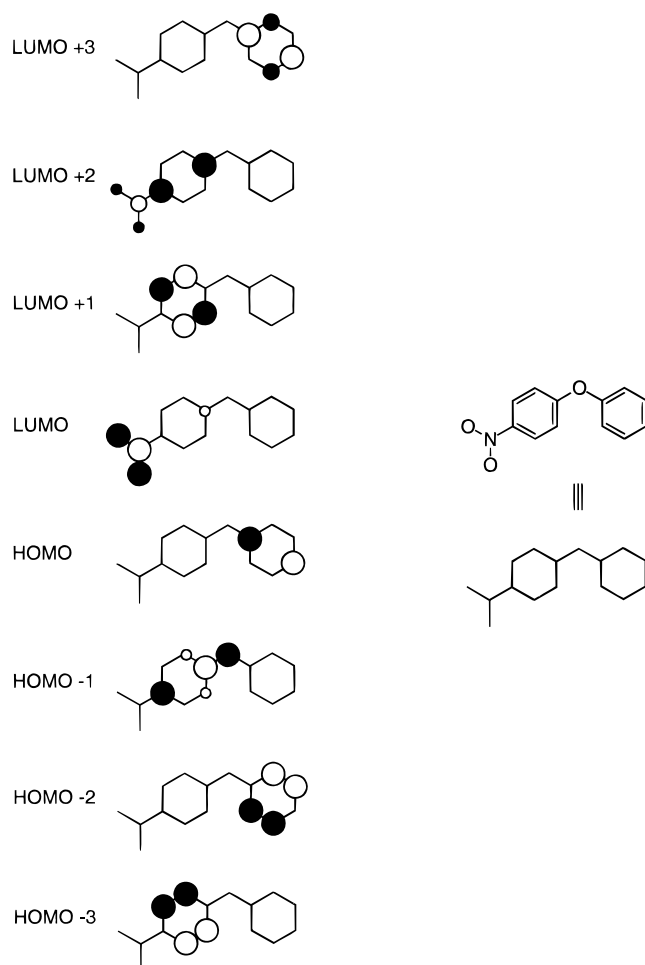
singlet state ^a	$\Delta\mu$ (D)	oscillator strength	energy		major transitions (fraction)
			eV	nm	
S ₄	10.9	0.483	4.202	295.0	HOMO -1 → LUMO (0.78) HOMO -2 → LUMO (0.15)
S ₉	3.99	0.163	5.723	216.6	HOMO → LUMO +3 (0.32) HOMO -1 → LUMO +2 (0.38)
S ₁₂	-2.52	0.179	6.006	206.4	HOMO -4 → LUMO (0.86)
S ₁₆	-2.02	1.290	6.448	192.3	HOMO -1 → LUMO +4 (0.24) HOMO -3 → LUMO +1 (0.29)
S ₁₉	1.91	0.705	6.624	187.2	HOMO -1 → LUMO +1 (0.24) HOMO -3 → LUMO +2 (0.34)
S ₂₀	-4.02	0.484	6.660	186.2	HOMO → LUMO +4 (0.13) HOMO -1 → LUMO +4 (0.19) HOMO -2 → LUMO +4 (0.21)
S ₂₁	-3.89	0.582	6.672	185.8	HOMO → LUMO +4 (0.15) HOMO -1 → LUMO +4 (0.21) HOMO -2 → LUMO +3 (0.39)
S ₂₃	18.4	0.204	6.883	180.1	HOMO -2 → LUMO +1 (0.65) HOMO -3 → LUMO +1 (0.10)
S ₂₄	0.47	0.255	6.979	177.7	HOMO -1 → LUMO +7 (0.18) HOMO -2 → LUMO +4 (0.15) HOMO -3 → LUMO +1 (0.16)
S ₂₅	0.92	0.230	6.982	177.6	HOMO -1 → LUMO +7 (0.23) HOMO -2 → LUMO +7 (0.15) HOMO -2 → LUMO +4 (0.15) HOMO -3 → LUMO +1 (0.12)
S ₃₁	0.24 ^b	0.108	7.345	168.8	HOMO -4 → LUMO +2 (0.88)

^a The singlet states correspond exactly as listed in the ZINDO/sum-over-states output (S₁ = ground state). All singlet states with oscillator strength >0.1 are listed. ^b Small change in magnitude, but large change in direction.

show a larger change in dipole moment between the ground state and the excited state ($\Delta\mu$) than *N*-methyl derivatives **2** or **3**). The comparison of *N*-phenyl-4-nitroaniline (**4**) with *N,N*-dimethyl-4-nitroaniline (**3**) provides further insight into the NLO response of these compounds. The larger hyperpolarizability of **4** ($\beta_{\mu, 1907 \text{ nm}} = 17 \times 10^{-30} \text{ cm}^5 \text{ esu}^{-1}$) compared to **3** ($\beta_{\mu, 1907 \text{ nm}} = 13 \times 10^{-30} \text{ cm}^5 \text{ esu}^{-1}$) cannot be rationalized on the basis of differences in the electronic absorption spectra: the absorption maxima of **4** ($\lambda_{\text{max}} 380 \text{ nm}$) and **3** ($\lambda_{\text{max}} 382 \text{ nm}$) (Table 2) are virtually identical. Again, the participation of the phenyl moiety in the excited state differentiates the NLO response of *N*-phenyl derivative **4** from *N,N*-dimethyl analog **3**.

Using simple concepts based on the two-level model, the IBM group attributed the enhancement of hyperpolarizability of diarylamino donors relative to dialkylamino donors in terms of an increase in $\Delta\mu$ (change in dipole moment between ground and excited states).¹⁰ Our analysis now provides detailed insight into the origin of this effect. These concepts (charge transfer, $\Delta\mu$) form the natural terminology used in conjunction with the two-level model,³⁻⁵ although the VAMP calculations suggest that additional excited states play a significant role.

Ethers 6-8. EFISH measurements establish that 4-nitrophenol (**6**), *O*-methyl-4-nitrophenol (**7**), and *O*-phenyl-4-nitrophenol (**8**) all exhibit small hyperpolarizabilities. In contrast to the amine cases, *O*-phenyl substitution produces a smaller increase in hyperpolarizability than *O*-methyl substitution (Table 1). Within the context provided by the experimental values for **1-8**, MOPAC, ZINDO, and VAMP calculations all provide qualitatively reasonable predictions for the trends in hyperpolarizability displayed by **1-8** (Table 2). Both MOPAC and VAMP, however, dramatically overestimate the influence of the *O*-phenyl substituent in **8**. For this reason, we rely primarily on the ZINDO computations to perform our analysis of the hyperpolarizabilities of **6-8**.

**Figure 3.** Molecular orbital diagram for *O*-phenyl-4-nitrophenol (**8**).

As in the case of the amines, the ZINDO calculations indicate that a single, low-energy excited state makes the dominant contribution to the intrinsic hyperpolarizability of 4-nitrophenol (**6**), *O*-methyl-4-nitrophenol (**7**), and *O*-phenyl-4-nitrophenol (**8**).⁴⁰ The computations reveal that these excited states are described predominantly in terms of excitation from the donor orbital to the acceptor orbital (Table 4). In each case, the donor orbital is localized primarily on the ether oxygen, and the acceptor orbital is localized on the nitroaryl moiety (Figure 3). In **6** and **7**, the donor orbital is the HOMO; in **8** it is the HOMO -1. The *O*-phenyl substituent does not contribute significantly to either the donor orbital or the acceptor orbital. Consequently, the phenyl substituent does not participate in charge transfer from oxygen to the nitroaryl acceptor, and does not provide significant enhancement of the hyperpolarizability. The enhancement in hyperpolarizability in going from **6** to **7** or **8** apparently occurs because both *O*-methyl and *O*-phenyl substituents cause a slight increase in the energy of the donor orbital (Figure 4).

Comparisons of Amines and Ethers. The preceding discussion describes the origin of substituent effects within the amine series (**1-5**) and within the phenol/ether series (**6-8**). We now address the origin of (i) the intrinsic difference in hyperpolarizability between amines and phenols/ethers and (ii) the differential substituent effects observed between the two series.

The intrinsic difference in hyperpolarizability between 4-nitroaniline (**1**) and 4-nitrophenol (**6**) is well understood in terms of the difference in electronegativity between the donor atoms (N vs O). In **1**, the HOMO lies at higher energy than in **6**

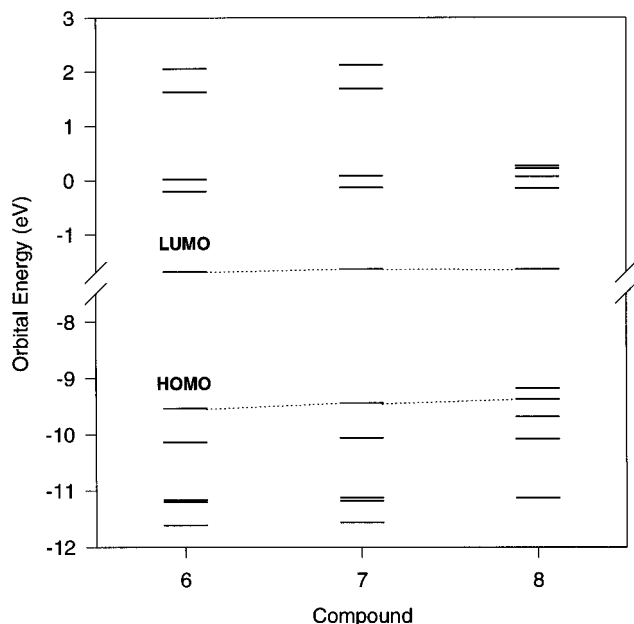


Figure 4. Computed energy levels (ZINDO) for frontier molecular orbitals of 4-nitrophenol (**6**), *O*-methyl-4-nitrophenol (**7**), and *O*-phenyl-4-nitrophenol (**8**).

(Figures 1 and 4). The smaller HOMO-LUMO separation in **1**, relative to **6**, provides greater mixing of ground state and excited state, which yields a larger molecular hyperpolarizability.

N-Phenyl substitution of 4-nitroaniline (**1**) produces a significant increase in hyperpolarizability, while *O*-phenyl substitution of 4-nitrophenol (**6**) produces a very small increase in hyperpolarizability. Our analysis traces this differential substituent effect to differences in the energies of the donor orbitals in *N*-phenyl-4-nitroaniline (**4**) and *O*-phenyl-4-nitrophenol (**8**) (*vide supra*). Moreover, the donor orbital (HOMO) in **4** contains phenyl character (Figure 2), while the donor orbital (HOMO -1) in **8** does not (Figure 3). These differences arise as a natural consequence of the molecular geometries (Figure 5). The structure of *N*-phenyl-4-nitroaniline (**4**) permits reasonable orbital overlap between the two aryl rings. The amine is nearly coplanar with the nitroaryl ring (sum of the angles at the amine = 355°), and the plane of the *N*-phenyl substituent makes a dihedral angle of approximately 50° with the plane of the nitroaniline ring. In contrast, the structure of *O*-phenyl-4-nitrophenol (**8**) does not permit significant orbital overlap between the two aryl rings (dihedral angle 90°). In comparing the structures of ether **8** and amine **4**, the shorter C—O bonds⁴² and the smaller C—O—C bond angle⁴² force the two aryl rings into closer proximity in **8**. This results in a larger dihedral angle between the rings and, consequently, poorer orbital overlap.

Implications Concerning Alternate Pathways for Extended Conjugation. In our opinion, one of the important lessons to evolve from this investigation concerns the analysis of the *N*-phenyl substituent as a means of extending the conjugation in nonlinear optical materials (*vide supra*). Consider the effect of extending the conjugation in 4-nitroaniline (**1**, D- π -A) by adding a C₆H₄ π -electron subunit (π'). Isomeric structures *N*-phenyl-4-nitroaniline (**4**, π' -D- π -A) and 4-amino-4'-nitrobiphenyl (**9**, D- π' - π -A) are possible. Compound **4** represents

(42) C_{phenyl}—O, 1.400 Å; C_{phenyl}—N, 1.409 Å; C_{aryl}—O, 1.382 Å; C_{aryl}—N, 1.388 Å; C—O—C angle, 116°; C—N—C angle, 124°. Computed values based on AM1-optimized geometry.

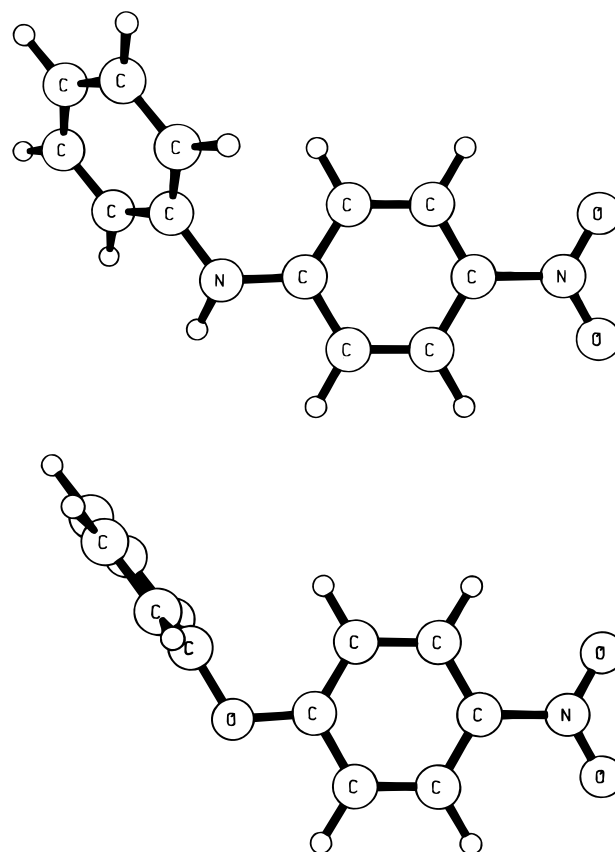
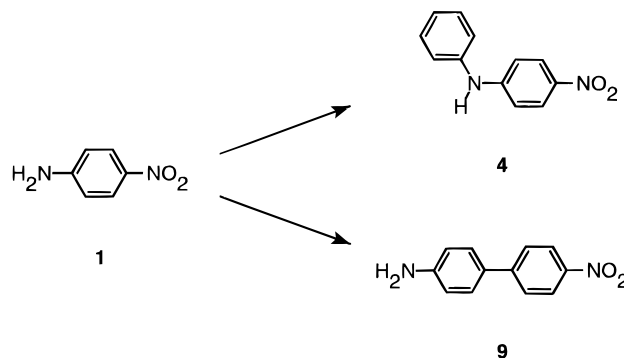


Figure 5. Computed geometries (AM1) for *N*-phenyl-4-nitroaniline (**4**, top) and *O*-phenyl-4-nitrophenol (**8**, bottom).

a “non-traditional” method of increasing the conjugation of **1**, because the additional π -electron subunit lies outside the donor—



acceptor framework. Interestingly, the experimental hyperpolarizability of *N*-phenyl-4-nitroaniline (**4**, $\beta_{\mu 1907} = 17 \times 10^{-30} \text{ cm}^5 \text{ esu}^{-1}$) exceeds that of 4-amino-4'-nitrobiphenyl (**9**, $\beta_{\mu 1907} = 14 \times 10^{-30} \text{ cm}^5 \text{ esu}^{-1}$).⁴³ This effect cannot be attributed to differences in the electronic absorption spectra of **4** and **9**.⁴⁴ This “non-traditional” substitution pattern of π -conjugation raises intriguing new possibilities concerning the design of

(43) Our value of $\beta_{\mu 1907} = 14 \times 10^{-30} \text{ cm}^5 \text{ esu}^{-1}$ for **9** in CHCl₃ differs from the value of $\beta_{\mu 1907} = 24 \times 10^{-30} \text{ cm}^5 \text{ esu}^{-1}$ measured by Cheng et al.^{19b} One significant discrepancy can be traced to the differing values of the dipole moment for **9**: 6.9 D (present work) vs 5.0 D (Cheng et al.). We typically observe reasonable agreement between our experimental dipole moments and those computed by AM1 (compare Tables 1 and 2). This agreement holds also for compound **9** (experimental 6.9 D; computed-AM1 7.6 D; computed-PM3 6.9 D³²).

(44) *N*-Phenyl-4-nitroaniline (**4**, $\lambda_{\text{max}} = 380 \text{ nm}$) and 4-amino-4'-nitrobiphenyl (**9**, $\lambda_{\text{max}} = 374 \text{ nm}$) display very similar absorption spectra in CHCl₃. The small blue-shift of **9** vs **4** suggests a slightly greater deviation from planarity for biphenyl **9** than for diphenylamine **4**.

second-order NLO chromophores; these issues will be considered in greater detail in subsequent publications.

Summary

Experimental measurements (EFISH) establish that *N*-phenyl substitution of 4-nitroaniline (**1**) produces a greater increase in molecular hyperpolarizability than *N*-methyl substitution. Theoretical analysis describes this unanticipated effect in terms of two factors: the larger perturbation in the energy of the donor orbital by the phenyl substituent, and the additional contribution of π -electron density from the phenyl substituent to the HOMO in **4**. This effect can be interpreted as an alternate method of increasing the π -conjugation length of a molecule. In the phenol/ether series, experimental measurements establish that *O*-phenyl substitution of 4-nitrophenol (**6**) produces a smaller increase in hyperpolarizability than *O*-methyl substitution. The differential behavior of amines and ethers toward phenyl substitution arises from inherent structural factors. The shorter C—O bond and smaller C—O—C angle force a larger dihedral angle between the aryl rings in diphenyl ether **8**. The *O*-phenyl substituent is effectively twisted out of conjugation with the donor—acceptor substituted π -system and therefore exerts only a small influence on the molecular hyperpolarizability.

Experimental Section

4-Nitroaniline (**1**), *N*-methyl-4-nitroaniline (**2**), *N*-phenyl-4-nitroaniline (**4**, 4-nitrodiphenylamine), 4-nitrophenol (**6**), *O*-methyl-4-nitrophenol (**7**, 4-nitroanisole), and *O*-phenyl-4-nitrophenol (**8**, 4-nitrodiphenyl ether) were purchased from Aldrich and purified by column chromatography prior to use. *N,N*-Dimethyl-4-nitroaniline (**3**),⁴⁵ 4-nitrotriphenylamine (**5**),⁴⁶ and 4-amino-4'-nitrobiphenyl (**9**)⁴⁷ were synthesized using literature procedures.

(45) Cardellini, L.; Greci, L.; Stipa, P.; Rizzoli, C.; Sgarabotta, P.; Ugozzoli, F. *J. Chem. Soc., Perkin Trans. 2* **1990**, *11*, 1929–1934.

(46) Herz, R. *Chem. Ber.* **1890**, *23*, 2536–2542.

Ground State Dipole Moment Measurements. Ground state dipole moments were determined from an analysis of the solution dielectric constant versus concentration of solute (10^{-2} to 10^{-3} M) using 1,4-dioxane as solvent. The dielectric constant of each solution was determined by measuring the differential capacitance of the solution using a Stanford Research Systems Model SR270 LCR meter and a two-terminal stainless steel electrode cell.^{16,48}

Electric-Field-Induced Second-Harmonic (EFISH) Generation.^{3–5} Hyperpolarizability measurements at 1064 nm were performed in 1,4-dioxane as described previously.^{16,48} Hyperpolarizability measurements at 1907 nm were performed using a series of solutions (10^{-2} to 10^{-3} M) of the solute in chloroform.⁴⁹

Acknowledgment. The National Science Foundation provided support for this project (Presidential Young Investigator Award CHE-8957529) and for the departmental computing facilities (CHE-9007850). We gratefully acknowledge additional funding from the 3M Corporation and the Alfred P. Sloan Foundation. We thank Professor Tim Clark (Erlangen) for providing his VAMP program and Dr. Max Muir (Molecular Simulations, Inc.) for computational assistance. C.M.W. thanks the Department of Education for a graduate fellowship, and K.L.K. thanks the Amoco Corporation for a graduate fellowship.

Supporting Information Available: Molecular orbital diagrams (AM1) for compounds **1–9**; tables of excited states which may contribute to hyperpolarizability for compounds **1–9** (data computed using both ZINDO and VAMP); table of physical constants used in the analysis of EFISH experiment (31 pages). See any current masthead page for ordering and Internet access instructions.

JA960284G

(47) (a) Gull, H. C.; Turner, E. E. *J. Chem. Soc.* **1929**, 491–500. (b) Idoux, J. P. *J. Chem. Soc.* **1970**, 435–437.

(48) Kott, K. L. Ph.D. Dissertation, University of Wisconsin—Madison, 1993.

(49) Whitaker, C. M. Ph.D. Dissertation, University of Wisconsin—Madison, 1995.